Chapter 2

Basic Principles

2.1 The Scanning Tunnelling Microscope

The Scanning Tunnelling Microscope (STM) was invented in 1981 by G. Binnig and H. Rohrer[33-35] and within a few years it emerged to one of the most widely used tools in surface science. The STM makes use of the quantum mechanical tunnel effect: A sharp metallic tip is positioned a few Angstrom (Å) over a conductive surface and a voltage in the order of 1 V is applied. The potential barrier between tip and surface is larger than the electrons energy, thus forbidding a current flow in the classical picture. Nevertheless, the electronic wave functions of tip and surface, decaying into the junction gap, overlap each other, leading to a finite probability of tunnelling for the electrons. The tunnel current is usually in the order of pico to nano Ampere and depends exponentially on the distance between tip and sample, changing about one order of magnitude with 1 Å change in the tip-sample distance.

In the typical working mode (called constant-current-mode) the tip is scanned line wise over a region of the surface and the tunnelling current is kept constant by regulating the tip height (z) through a feedback loop. A map of the surface is obtained by assigning to each lateral x/y-position of the scanned region the tip height $z(x,y)$. In this mode the tip follows roughly the corrugation of the surface, creating a nearly topological map. However, the STM image is also influenced by electronic effects. More precisely the tip moves on a surface of constant local density of states (LDOS) close to the Fermi energy. In general it is not trivial to distinguish between topologic and electronic effects.

In order to achieve high spatial resolution, the demands on stability and precision of the tip movement are extreme. For the tip positioning, piezoelectric crystals, called piezos in the following, are employed. These are materials which deform in dependence on the applied voltage. For the used piezos at temperatures of about 7 K, the elongation is in the order of 10 Å/V and the maximum voltage that can be transformed into an elongation is about 100 V. Therefore the maximal scan area is in the order of 1 μm^2. The spatial resolution is not limited by the piezos, but by electronic and mechanic noise. Much effort has to be done to decouple the STM against mechanical oscillations: Our STM hangs at springs and is damped by an eddy current break. Furthermore, the whole STM chamber rests on pneumatically damped feet. Typically the lateral resolution of a Low Temperature-STM (LT-STM) is in the order of 1 Å and the vertical resolution is in the order of 1 pm = 0.01 Å.

There are several benefits of working at low temperatures, which are important for this work. Due to decreased thermal drift, the STM is very stable and due to lower thermal noise, the energy resolution is increased. The latter property is important for Scanning Tunnelling Spectroscopy (STS). Moreover, due to the cold environment surrounding the sample (the cold shields are working as cryo-pumps), the vacuum conditions are improved. Furthermore, adsorbates with low diffusion barriers can only be imaged at low temperatures, when their surface diffusion is frozen in.

2.2 Theoretical Description of the Tunnelling Process

A variety of theories have been developed to describe the tunnelling process taking place in STM. The fundamental works will be briefly reviewed in the following. In a first schematic approach, the tunnel-effect is treated one-dimensionally and time-independent. In this approximation, the problem can be solved analytically. The elastic tunnelling of an electron of energy E through a constant potential barrier V_0 can be described by a stationary Schrödinger equation:

$$\left[\frac{1}{2m}\left(\frac{\hbar}{i}\frac{\partial}{\partial x}\right)^2 + V(x)\right]\Psi(x) = E\Psi(x)\,. \tag{2-1}$$

Inside the metal, the electron is treated as a free particle, while in the tunnelling region (barrier of length s) the potential is higher than the energy of the electron:

$$\begin{aligned} V(x) &= 0 \quad \text{for } x \notin [0,s] \quad \text{(inside the metal)},\\ V(x) &= V_0 \quad \text{for } x \in [0,s] \quad \text{(inside the barrier)}. \end{aligned} \tag{2-2}$$

The solutions have the form:

$$\Psi(x) = \exp\left(\pm i\,k\,x\right) \quad \text{with } k = \sqrt{\frac{2m(E)}{\hbar^2}} \quad \text{for } x \notin [0,s] \text{ and} \tag{2-3}$$

$$\Psi(x) = \exp\left(\pm \kappa\,x\right) \quad \text{with } \kappa = \sqrt{\frac{2m(V_0 - E)}{\hbar^2}} \quad \text{for } x \in [0,s]. \tag{2-4}$$

An incident wave is partly reflected and partly transmitted by the barrier and the transmission coefficient T can be determined by wave-matching of the amplitude and the first derivative. Energy diagram and wave functions are shown schematically in Fig. 2.1. For the transmission coefficient one obtains:

$$T = \frac{1}{1 + \frac{\left(k^2 + \kappa^2\right)^2 \sinh^2(ks)}{4k^2\kappa^2}} \quad . \tag{2-5}$$

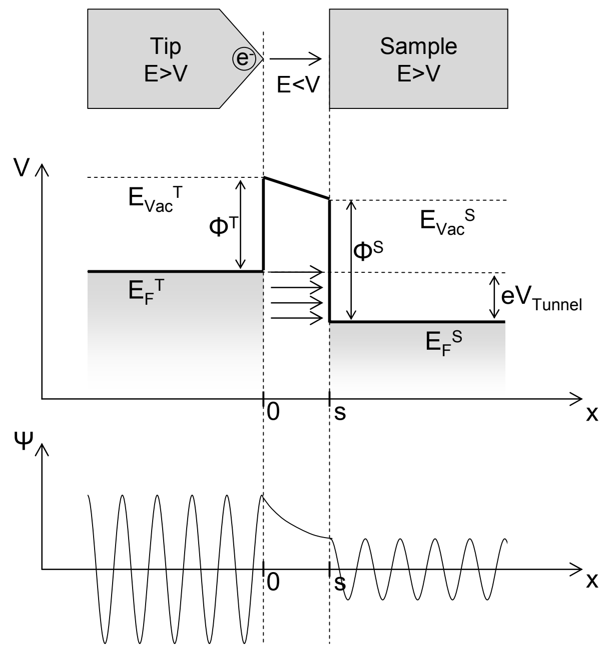

Fig. 2.1. Schematic Energy diagram and wave functions in one dimension, in case of electrons tunnelling from the tip to the sample. $E_F^{T/S}$ are the tip/sample Fermi energies, $E_V^{T/S}$ are the tip/sample vacuum levels, and $\Phi^{T/S}$ are the tip/sample work functions, respectively. V_{Tunnel} is the tunnelling bias. For simplicity only the real part of the wave functions is shown.

For a large barrier ($s\kappa$>> 1), T can be approximated[36] as

$$T \approx \frac{16k^2\kappa^2}{\left(k^2 + \kappa^2\right)^2} \exp\left(-2\kappa s\right) \quad . \tag{2-6}$$

This result shows the exponential relation between transmission coefficient and tunnelling distance *s* and yields to the exponential dependence of the tunnelling current, which is proportional to the transmission coefficient, on the tip-sample distance. This exponential dependence is the fundament for the high spatial resolution of the scanning tunnelling microscope.

In the WKB approximation (Wentzel, Kramers, Brillouin, 1926) the solution can be expanded to a non-constant potential V(x), yielding the transmission coefficient

$$T \cong \exp\left\{-\frac{2}{\hbar}\int_0^s \sqrt{2m[V(x)-E]}dx\right\}. \tag{2-7}$$

However, a three-dimensional treatment is required to describe the tunnelling geometry, as shown by Bardeen[37], who treated the problem as a time-dependent perturbation. The transmission probability from an unperturbed state on one side of the barrier to an unperturbed state on the other side, considering the tunnelling region as a perturbation, is calculated in analogy to Fermis Golden rule. The transition probability from the tip state Ψ_t to the sample state Ψ_s is called the tunnelling matrix element M_{ts}:

$$M_{ts} = \frac{-\hbar^2}{2m}\int dS \cdot (\Psi_t^* \nabla \Psi_s - \Psi_s \nabla \Psi_t^*). \tag{2-8}$$

The integration is done over a surface S between tip and sample, through which the entire tunnelling current flows. The transition rate is $|M_{ts}|^2$. For the tunnelling current one obtains:

$$I = \frac{2\pi e}{\hbar}\sum_{t,s} \left\{f(E_t)\,(1-f(E_s+eV)) - f(E_s+eV)\,(1-f(E_t))\right\} \times |M_{ts}|^2 \delta(E_t - (E_s - eV)) \ , \tag{2-9}$$

where $f(E)$ are the Fermi functions and E_t and E_s are the energies of the unperturbed wave functions of tip and sample, respectively. The Fermi functions enter here because only tunnelling from an occupied to an unoccupied state is allowed. As electrons can tunnel in both directions, from tip to sample and from sample to tip, partly compensating each other, the tunnelling matrix element has to be summed over all possible tip and sample states. The delta function is expression of energy conservation during the tunnelling process.

Starting from Bardeens theory, Tersoff and Hamann[38, 39] calculated the tunnelling current in case of STM and allowed the theoretical interpretation of STM images. They assumed the relatively simple geometry of a spherical tip and a plane substrate (Fig. 2.2), therefore using s-like wave-functions (angular momentum quantum number $l = 0$) for the tip.

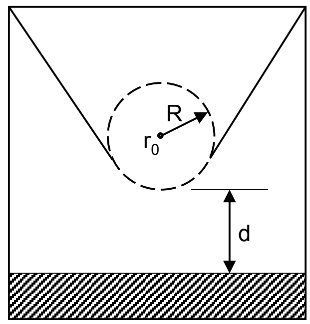

Fig. 2.2. Schematic picture of tunnelling geometry in the Tersoff-Hamann model. The probe tip has arbitrary shape but is assumed locally spherical with a radius of curvature *R*, where it approaches nearest the surface. The distance of nearest approach is *d*. The centre of curvature of tip is $\vec{r}_0$.[38]

In the limit of small voltage $(V \to 0)$ and low temperature $(T \to 0)$ Eq. (2-9) reduces to:

$$I = \frac{2\pi e^2}{\hbar} V \sum_{t,s} \left|M_{ts}\right|^2 \delta(E_s - E_F)\ \delta(E_t - E_F)\,, \qquad \text{(2-10)}$$

where E_F is the Fermi energy. However, to calculate the tunnelling matrix element, the wave-functions of sample and tip have to be defined. The sample wave-function is assumed to decay exponentially outside the metal and to propagate freely parallel to the surface:

$$\Psi_s = \Omega_s^{-1/2} \sum_{\vec{G}} a_{\vec{G}} \exp\left(-\sqrt{\kappa^2 + \left|\vec{k}_{\|} + \vec{G}\right|^2} \cdot \vec{r}_{\perp}\right) \cdot \exp\left(-\sqrt{i\ \left(\vec{k}_{\|} + \vec{G}\right)^2} \cdot \vec{r}_{\|}\right) \qquad \text{(2-11)}$$

$$\text{with } \kappa = \frac{\sqrt{2m\Phi}}{\hbar}\,, \qquad \text{(2-12)}$$

where Ω_s is the volume of the sample and $\vec{G}$ is the reciprocal lattice vector. The decay rate κ outside the metal depends on the work function of the metal Φ.

The s-like wave function of the spherical tip with radius R at position $\vec{r}_0$ (for the definition of R and $\vec{r}_0$ see Fig. 2.2) is:

$$\Psi_t = \Omega_t^{-1/2} c_t \frac{\kappa\ R \cdot \exp(\kappa\ R)}{\kappa\ |\vec{r} - \vec{r}_0|} \cdot \exp(\kappa\ |\vec{r} - \vec{r}_0|), \tag{2-13}$$

where c_t is a normalisation parameter in the order of 1. Now the matrix element according to Eq. (2-8) can be calculated:

$$M_{ts} = \frac{2\pi\hbar^2}{m} \Omega_t^{-1/2} R \cdot \exp(\kappa\ R) \sum_s \left| \Psi_s(\vec{r}_0)^2 \right| \delta(E_s - E_t)\ . \tag{2-14}$$

Using expression (2-10) the tunnelling current is evaluated. One obtains:

$$I = \frac{32\pi^3 e^2\, V\, \Phi^2 R^2 \exp(2\ \ \kappa\ R)}{\hbar \kappa^4} D_t\,(E_F) \cdot \sum_s \left| \Psi_s(\vec{r}_0)^2 \right| \delta(E_s - E_t), \tag{2-15}$$

where $D_t\,(E_F)$ is the density of states per unit volume of the tip at the Fermi energy E_F. The sum in (2-15) is identified as the local density of states at E_F of the sample at the position of the tip. This is often referred to as Local Density Of States (LDOS):

$$\rho(\vec{r}_0, E_F) \equiv \sum_s \left| \Psi_s(\vec{r}_0)^2 \right|\ \ \delta(E_s - E_t). \tag{2-16}$$

Substituting typical values in (2-15) one obtains

$$I = 0.1 R^2\, V \exp\left(2\kappa R\right)\ \rho(\vec{r}_0, E_F), \tag{2-17}$$

where the distance is in a. u. and energy in eV. This result means that the STM is measuring the contour of constant LDOS of the sample. Since

$$\left|\Psi_s(\vec{r}_0)\right|^2 \propto \exp\left(-2\kappa\ (R+s)\right), \tag{2-18}$$

one obtains once again the exponential distance dependence for the tunnelling conductance σ, i.e.

$$\sigma \propto \exp\left(-2\kappa s\right), \tag{2-19}$$

$$\text{with } \kappa = \frac{\sqrt{2m\Phi}}{\hbar}. \tag{2-20}$$

Substituting a typical metal work function of $\Phi = 4.5$ eV, one can estimate the tunnelling resistance as

$$R \propto \exp(A \cdot s), \tag{2-21}$$

With A = 2.18 and s in Å, showing that R increases approximately one order in magnitude, when s increases 1 Å. In combination with the contact resistance R_0 (corresponding to $s = 0$), which can be experimentally measured, the tip height can be approximately estimated for a given tunnelling resistance, obtaining

$$s \approx \log\left(\frac{R}{R_0}\right), \tag{2-22}$$

with s in Å, where the contact resistance on metal surfaces is typically $R_0 \approx 10$ kΩ.[40]

2.3 Scanning Tunnelling Spectroscopy

By means of Scanning Tunnelling Spectroscopy (STS) it is possible to study the electronic properties of the surface locally. The idea is to measure the LDOS not only at the Fermi level, but at any given energy.

The problem of STS can be discussed in an abstract form to avoid the complications of the specific forms of the wave functions in equation (2-8).[41] The sum over participating states in equation (2-10) implies an energy integral. Thus the tunnelling current will be the sum over terms each of them has the form

$$I(eV) \propto \int_0^{eV} D_t(E-eV)\ D_s(E)\ dE\,, \tag{2-23}$$

where D_t and D_s are the tip and sample density of states, respectively. In an one-dimensional model[42, 43] dI/dV is given by

$$\frac{dI}{dV} \ \propto\ D_t(0)\ D_s(eV)\ +\int_0^{eV} D_s(E)\frac{D_t(eV-E)}{dV}dE\,. \tag{2-24}$$

The first term is a counting term that arises because a variation in the bias voltage V changes the interval over which tunnelling can occur, i.e. the number of states which are involved. The integral term considers that the two functions are pinned to their respective Fermi energies, so that they are shifted relative to each other when the voltage is changed. Under the common assumption of a featureless tip, i.e. constant D_t, the integral vanishes and dI/dV can be interpreted as a good measure of $D_s(eV)$, i.e. the density of states of the sample at $E = eV$.[44]

The first derivative of I with respect to V can be directly measured with the STM using lock-in technique. A small AC signal of amplitude V_{mod} and frequency ω is superposed to the tunnelling bias V_0 and the lock-in amplifier works as a band pass filter, measuring the amplitude of the tunnelling current that is oscillating with ω. The amplitude of the first harmonic is proportional to the differential conductance dI/dV for small modulation signals V_{mod}, as can be seen from the Taylor expansion of the current with tunnelling bias $V(t) = V_0 + V_{mod} \times \cos(\omega t)$:

$$I\left(V_0 + V_{\mathrm{mod}}\cos(\omega\, t)\right) =$$

$$I_0 \ +\ \frac{dI(V_0)}{dV}\cdot V_{\mathrm{mod}}\cdot\cos(\omega\, t)\ +\ \frac{d^2 I(V_0)}{dV^2}\cdot V_{\mathrm{mod}}^2\cdot\cos^2(\omega\, t)\ +\ \ldots \tag{2-25}$$

The lock-in signal $\frac{dI(V_0)}{dV} \cdot V_{\text{mod}}$ can be measured at a chosen point of the sample, ramping the voltage V_0 with the feedback loop switched off, yielding the spectral density of states at this point. On the other hand, the surface can be scanned at a certain voltage V_0 and, by recording the lock-in signal at each point, one yields a so called *dI/dV*-map of the surface, i.e. a map of the LDOS of the surface at energy $E = eV_0$.

The amplitude of the second harmonic in (2-25), which oscillates with ω^2, is used for inelastic tunnelling spectroscopy (IETS). In this case, processes where the tunnelling electrons loose energy (e.g. by exciting vibrational[45-47] or rotational[48] modes) can be investigated.

2.4 STM induced Manipulation

Soon after the first STM experiments it was realized that the tip often modifies the substrate because of the close proximity to the surface atoms. This obvious disadvantage for imaging turned into a positive prospect by realizing that the modifications can be performed in a controlled way[4, 20]. At low temperature, the tip of the STM can be used to build atomically precise structures and to investigate the motion of single atoms and molecules.

There are two basic techniques which allow the transport of atoms and small molecules with the STM tip in order to build nanostructures. Either single particles are moved by the tip on the surface, without loosing contact to it (lateral manipulation), or single particles are picked up by the tip and are deposited at the desired location (vertical manipulation).

The tip-sample interactions used for this purpose can be divided into two broad categories: Forces that act on the sample because of the proximity of the tip even in absence of bias voltage and effects caused by the applied bias voltage, i.e. electric field and tunnelling current through the gap region.[49] For the lateral manipulation at atomic scale, the interaction forces between tip and atom, i.e. van der Waals or chemical forces, are sufficient to move atoms and no electric field or tunnelling current has to be applied. For vertical manipulation, however, field and current effects play a major role. Both types of manipulation were used for the first time by the group of Eigler at IBM-Almaden[4, 19] and then by Meyer et al. at the FU-Berlin[21, 50] to build nanostructures from single atoms and molecules.

An example of an atomically defined nanostructure, which has been built by lateral manipulation by Crommie et al. [51], is shown in Fig. 2.3. In this case single Fe atoms have been arranged in the shape of a circle on Cu(111) in order to study the confinement and scattering of the surface state electrons inside the so called quantum corral.[51]

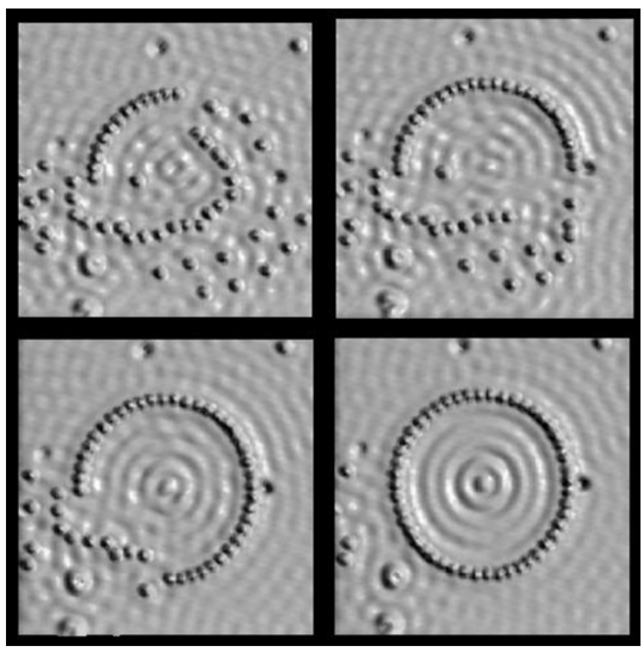

Fig. 2.3. Different stages during the construction of a quantum corral built from 48 Fe adatoms on Cu(111) by means of lateral STM manipulation. Confined electron states give rise to standing wave patterns. Tunnelling parameters: V = 10 mV, I = 1.0 nA, T = 4 K. The diameter of the corral is 143 Å. From ref. [51]

In order to laterally manipulate an atom, the tip is first positioned above the atom and the tip-sample distance is reduced to typically 1-3 Å. Therefore the tunnelling resistance R is lowered from typical scanning parameters (R in the range of

10^7 - 10^{11} Ω) into the regime of 10^4 - 10^6 Ω. The relation between tip-sample distance and *R* is approximately determined by Eq. (2-22). The tip is moved from the initial position of the adsorbate to the desired final position with the chosen manipulation parameters. The area is subsequently scanned again with imaging parameters to observe the outcome of the manipulation attempt.

During manipulation, the tip height is recorded as a function of lateral movement and called the manipulation signal. Different forms of lateral manipulation can be recognized by the typical shape of the manipulation signal.[52] It can be distinguished between three modes, corresponding to different lateral motion of the particle. Typical manipulation signals are shown schematically in Fig. 2.4 and the manipulation modes are explained in the following:

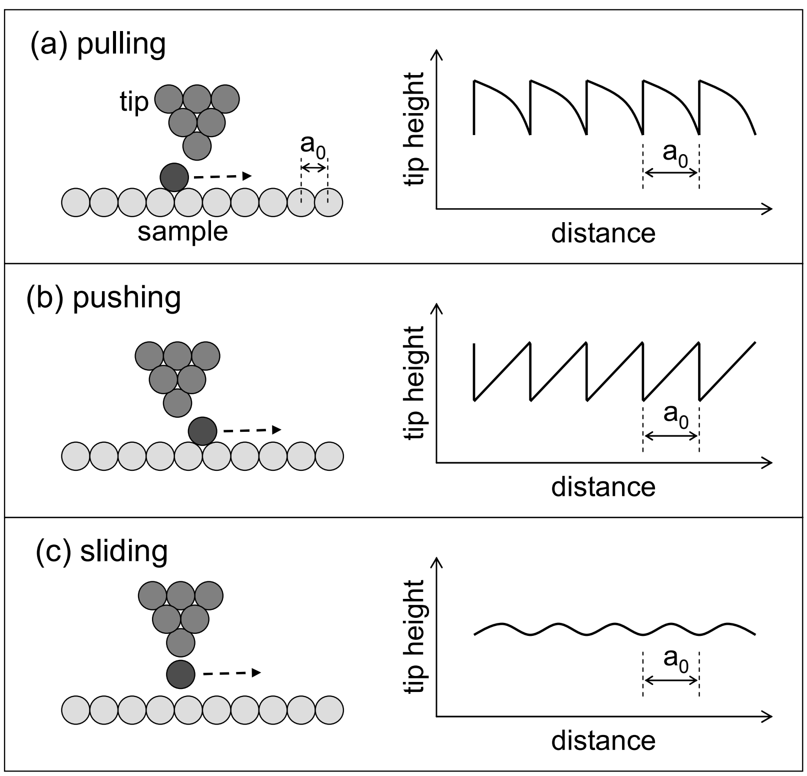

Fig. 2.4. Schematic representation of the different manipulation modes and their characteristic manipulation signals: (a) pulling, (b) pushing, (c) sliding. The Lattice parameter is a_0. The dashed arrows indicated the direction of manipulation.

- Pulling mode (Fig. 2.4(a)): Attractive forces, usually addressed to van der Waals interaction, between adsorbate and tip force the adsorbate to follow the motion of the tip. When the tip approaches the molecule, the tip height immediately rises because the adsorbate jumps under the tip due to the attractive forces. Then the tip height drops with finite slope when the tip moves away from the adsorption site of the molecule, following the contour of constant LDOS of the adsorbate and surface, until the molecule jumps again to an adsorption position underneath the tip (and the tip again retracts). The periodicity of the signal corresponds to the adsorption positions along the path of the adsorbate. In this mode the adsorbate stays behind the tip with respect to the manipulation direction.

- Pushing mode (Fig. 2.4(b)): Repulsive interaction between STM tip and adsorbate forces the molecule to jump away from the tip if the tip-adsorbate distance decreases below a critical value. In this case the typical manipulation signal has typically the form of a saw-tooth, but inverted with respect to the case of manipulation in pulling mode. The tip height rises with finite slope, when the tip is approaching the molecule. Then it suddenly drops, when the molecule jumps away from the tip, explaining the manipulation signal of Fig. 2.4(b). In this mode the adsorbate is positioned in front of the tip with respect to the manipulation direction.

- Sliding mode (Fig. 2.4(c)): An adsorbate is moved in sliding mode when the tip-particle interaction is so strong that tip and particle move together on the surface. In this case the adsorbate-tip distance remains nearly constant during the manipulation process. The manipulation signal is smooth and reflects the corrugation of the surface, which is scanned by the adsorbate at the tip apex. To manipulate single atoms in sliding mode, the tip to sample distance has normally to be further decreased with respect to the parameters used for pulling the molecule.

Specially designed large organic molecules have been successfully manipulated at room temperature by Jung et al.[53], but to obtain quantitative information about the manipulation process, the stability and the low noise level achievable by LT-STM are necessary. Moresco et al. have shown that the manipulation signal of a large organic molecule with internal degrees of freedom can be influenced by the deformation of the molecule, e.g. by the bending or the rotation of internal chemical bonds.[54] Large molecules have been successfully manipulated in the so called "constant height manipulation mode", recording manipulation signals.[55] In this mode the feedback loop is switched off during the manipulation process, hence the tip-sample distance is kept constant, avoiding instabilities in the vertical position of the tip. In this case, the tunnelling current is recorded during the manipulation process, serving as manipulation signal. By comparison with calculated manipulation signals, the contributions of different molecular parts can be distinguished and the internal deformation of the molecule during manipulation can be determined.[54, 56]

Another form of STM induced manipulation is the change of internal conformations of a molecule. In this case the tip is moved above the adsorbate with imaging parameters and then the tip-sample distance, bias voltage, and tunnelling current are altered in order to perform the manipulation. The manipulation can result not only in a molecular motion[4, 45], but furthermore chemical reactions[57-59], molecular desorption[60, 61], the charging of an adatom[62] or the change of the internal molecular conformation[7, 63, 64] have been reported.

STM induced manipulation is a central technique in this work for two reasons: On the one hand manipulation of molecules is used to form artificial structures necessary for further investigation, like the contact of a Lander molecule to a mono-atomic step edge described in chapter 5. On the other hand, manipulation experiments are performed to reveal information about the mechanical deformation of the molecule, the movement path, the molecular-substrate interaction, and the tip-molecular interaction.

2.5 Elastic Scattering Quantum Chemistry

Different theoretical approaches for the calculation of STM images of organic molecules on conducting surfaces have been presented within the last years. Contour maps of constant probability density of the HOMO (Highest Occupied Molecular Orbital) and the LUMO (Lowest Unoccupied Molecular Orbital) of molecules have been extensively used to interpret STM images of adsorbates.[65, 66] However, this interpretation does not take into account the shifting of molecular orbitals in the presence of the metallic surface. More sophisticated models use either the Tersoff-Hamann approximation, valid however only for large tip-molecule separation[38, 39], or more generally the Bardeen approach[37], modelling the surface by the jellium model[67, 68]. However, none of these methods takes into account the mechanical deformation of the molecule under the influence of the STM tip.

The image calculations shown in this work are based on the Elastic Scattering Quantum Chemistry (ESQC) method, developed by Sautet and Joachim.[69, 70] This approach takes into account the full geometry of tip, adsorbate, and sample. The tunnelling of an electron is treated as a scattering event. The tunnelling gap represents a defect which breaks the translational invariance of the tip-bulk and the substrate-bulk, and therefore scatters the incoming tunnelling electron. Electron-electron and electron-phonon coupling are both ignored and the scattering event is assumed to be elastic.

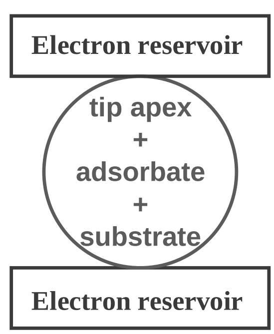

Fig. 2.5. Schematic representation of the junction “tip-apex-adsorbate-substrate” (TAS) and the connection to the electron reservoirs of the bulk of the tip and the sample as considered for the ESQC method.

A matrix representation of the Hamiltonian is constructed, which takes into account the complete chemical description of tip, adsorbate, and substrate. The Hamiltonian can be constructed using tight-binding approximation, extended Hückel, Hartree-Fock, and density functional theory (DFT). In the case of the Lander molecules, requiring a large unit cell and a large amount of orbitals that must be taken into account, extended Hückel calculations are mainly used. The whole system can be represented by a model system of the form *...PPPDPPP...*, where *P* symbolizes a periodically repeated cell and *D* a defect cell. In this case *D* contains the whole scattering region called TAS (tip apex, adsorbate, and the first atom layers of the substrate). Tip apex and substrate surface are connected each to an electron reservoir, which is the metal bulk. Tip and sample are both assumed to be of the same material in this approach (both are modelled by cell *P*). Due to lateral cyclic boundary conditions the band structure of tip and substrate is obtained.

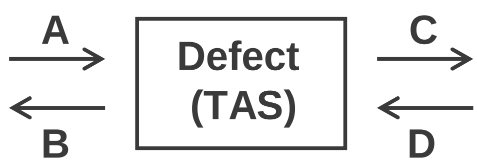

Fig. 2.6. Schematic picture of the scattering process at the tip-apex-adsorbate-substrate (TAS). Incoming (*A,D*) and outgoing (*B,C*) wave amplitudes in case of the matrix representation.

An useful tool to extract the electronic transmission is the scattering matrix *S(E),* which relates the amplitudes of the outgoing waves to those which are incoming on the defect (Fig. 2.6):

$$\begin{pmatrix} C \\ B \end{pmatrix} = S(E) \begin{pmatrix} A \\ D \end{pmatrix}. \qquad (2\text{-}26)$$

The transfer matrix *T(E)* relates the amplitudes on the far left side to those on the far right side (corresponding to Fig. 2.6)

$$\begin{pmatrix} C \\ D \end{pmatrix} = T(E) \begin{pmatrix} A \\ B \end{pmatrix}. \tag{2-27}$$

For the one-dimensional single impurity problem (i.e. only one channel) the T matrix has the following structure[70]:

$$T(E) = \begin{pmatrix} F(E) & G^*(E) \\ G(E) & F^*(E) \end{pmatrix} . \tag{2-28}$$

The transfer matrix is related to the scattering matrix by

$$S(E) = \frac{1}{F^*(E)} \begin{pmatrix} 1 & G^*(E) \\ -G(E) & 1 \end{pmatrix} , \tag{2-29}$$

then the transmission coefficient *t(E)* of an electron of energy *E* is

$$t(E) = \frac{|C|^2}{|A|^2} = \frac{1}{|F(E)|^2} \quad . \tag{2-30}$$

For more then one channel S and T are $2N \times 2N$ matrices and the problem has to be treated as shown in [71]. A general review of random-matrix theory on quantum transport is given in[72].

At low bias voltage the conductance is related to the transmission coefficient by the generalized Landauer formula[73]:

$$\frac{I}{V} = \frac{e^2}{\pi \hbar} t(E_F) , \tag{2-31}$$

where $t(E_F)$ is the transmission coefficient for an electron at Fermi energy E_F when no bias voltage is applied. The tunnelling current *I* at voltage *V* can now be calculated at any tip position *(x,y,z)*, and from the three-dimensional map of *I(x,y,z)*, a two-dimensional map of constant current or constant height can be calculated, simulating an STM image.

The ESQC calculations shown in this work have been performed in the group of C. Joachim at the Nanoscience Group, CEMES-CNRS, Toulouse. In this case the tip apex and the sample in the TAS are modelled by five layers of Cu atoms, which are arranged in a pyramidal shape in case of the STM tip. In case of a Lander molecule several hundred molecular orbitals are taken into account for the calculation of the transfer matrix.

To study the deformation of the molecule in the presence of the tip, Molecular Mechanics (MM) calculations have been employed.[74] MM calculations are a semi-empirical standard method of modelling a molecular geometry using Newtonian mechanics. Potential functions are used, which are optimised to fit a range of physical properties of a set of molecules. The geometry of the system is calculated by finding the energy minimum. Contrary to the ESQC method, MM calculations are conceptually simple and computationally inexpensive. The MM and ESQC methods have been combined making it possible to optimise the geometry of the molecule in the presence of sample and tip at each point of an ESQC simulated image. Therefore the images, which are calculated with this combined MM+ESQC technique, do take into account the deformation of the molecule due to the STM tip. Moreover, with the MM+ESQC technique it is possible to simulate the manipulation signal in case of STM induced lateral manipulation. The latter, however, is computationally very expensive: The calculation of a manipulation signal of a molecule in the size of a Lander takes about one week, using state of the art computing facilities.